Accepted Manuscript

Synthesis, antioxidant and antichagasic properties of a selected series of hydroxy-3-arylcoumarins

Natalia Robledo-O'Ryan, Maria João Matos, Saleta Vazquez-Rodriguez, Lourdes Santana, Eugenio Uriarte, Mauricio Moncada-Basualto, Francisco Mura, Michel Lapier, Juan Diego Maya, Claudio Olea-Azar

PII: S0968-0896(16)30742-8
DOI: http://dx.doi.org/10.1016/j.bmc.2016.11.033
Reference: BMC 13400

To appear in: *Bioorganic & Medicinal Chemistry*

Received Date: 16 September 2016
Revised Date: 30 October 2016
Accepted Date: 17 November 2016

Please cite this article as: Robledo-O'Ryan, N., João Matos, M., Vazquez-Rodriguez, S., Santana, L., Uriarte, E., Moncada-Basualto, M., Mura, F., Lapier, M., Diego Maya, J., Olea-Azar, C., Synthesis, antioxidant and antichagasic properties of a selected series of hydroxy-3-arylcoumarins, *Bioorganic & Medicinal Chemistry* (2016), doi: http://dx.doi.org/10.1016/j.bmc.2016.11.033

Graphical Abstract

To create your abstract, type over the instructions in the template box below.
Fonts or abstract dimensions should not be changed or altered.

Synthesis, antioxidant and antichagasic properties of a selected series of hydroxy-3-arylcoumarins

Leave this area blank for abstract info.

Natalia Robledo-O´Ryan,[a] Maria João Matos,[b]* Saleta Vazquez-Rodriguez,[b] Lourdes Santana,[b] Eugenio Uriarte,[b] Mauricio Moncada-Basualto,[a,c] Francisco Mura,[a] Michel Lapier,[d] Juan Diego Maya,[d] Claudio Olea-Azar[a]*

[a] *Free Radical and Antioxidants Laboratory, Inorganic and Analytical Department, Faculty of Chemical and Pharmaceutical Sciences, University of Chile, Sergio Livingstone Polhammer 1007, Independencia, Santiago, Chile.*

[b] *Department of Organic Chemistry, Faculty of Pharmacy, University of Santiago de Compostela, Santiago de Compostela, Spain.*

[c] *Department of Environmental Sciences, Faculty of Chemistry and Biology, University of Santiago of Chile, Santiago, Chile.*

[d] *Department of Molecular Pharmacology and Clinical, Faculty of Medicine, University of Chile, Santiago, Chile.*

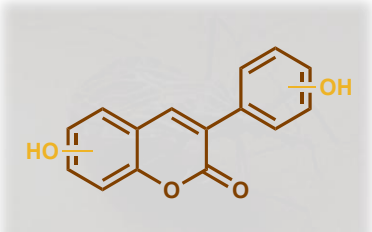

Bioorganic & Medicinal Chemistry
journal homepage: www.elsevier.com

Synthesis, antioxidant and antichagasic properties of a selected series of hydroxy-3-arylcoumarins

Natalia Robledo-O´Ryan,[a] Maria João Matos,[b]* Saleta Vazquez-Rodriguez,[b] Lourdes Santana,[b] Eugenio Uriarte,[b] Mauricio Moncada-Basualto,[a,c] Francisco Mura,[a] Michel Lapier,[d] Juan Diego Maya,[d] Claudio Olea-Azar[a]*

[a] *Free Radical and Antioxidants Laboratory, Inorganic and Analytical Department, Faculty of Chemical and Pharmaceutical Sciences, University of Chile, Sergio Livingstone Polhammer 1007, Independencia, Santiago, Chile.*
[b] *Department of Organic Chemistry, Faculty of Pharmacy, University of Santiago de Compostela, Santiago de Compostela, Spain.*
[c] *Department of Environmental Sciences, Faculty of Chemistry and Biology, University of Santiago of Chile, Santiago, Chile.*
[d] *Department of Molecular Pharmacology and Clinical, Faculty of Medicine, University of Chile, Santiago, Chile.*

ARTICLE INFO

Article history:
Received
Received in revised form
Accepted
Available online

Keywords:
Hydroxy-3-arylcoumarins
Antioxidant activity
Trypanosome
Chagas disease

ABSTRACT

Oxidative stress is involved in several parasitic diseases such as Chagas. Agents able to selectively modulate biochemical processes involved in the disease represent promising multifunctional agents for the delay or abolishment of the progression of this pathology. In the current work, differently substituted hydroxy-3-arylcoumarins are described, exerting both antioxidant and trypanocidal activity. Among the compounds synthesized, compound **8** showed the most interesting profile, presenting a moderate scavenging ability for peroxyl radicals (ORAC-FL=2.23) and a high degree of selectivity toward epimastigotes stage of the parasite *T. cruzi* (IC_{50} = 1.31 µM), higher than Nifurtimox (drug currently used for treatment of Chagas disease). Interestingly, the current study revealed that small structural changes in the hydroxy-3-arylcoumarin core allow modulating both activities, suggesting that this scaffold has desirable properties for the development of promising classes of antichagasic compounds.

* Corresponding author. Tel.: +34 981 528070; e-mail: mariacmatos@gmail.com; colea@uchile.cl

1. Introduction

Chagas' disease or American trypanosomiasis is a parasitic disease produced by a flagellated protozoo called *Trypanosoma cruzi* (*T. cruzi*), that represents a major health problem in South, Central and North America (Mexico and the south of the U.S.A.). However, during the last decade this disease has been spread to some non-endemic areas, driving this situation to a worldwide public health problem. According to statistics of PAHO (Pan American Health Organization) and WHO (World Health Organization), 7.7-10 million people are chronically infected with *T. cruzi*, and about 10,000-14,000 deaths per year are caused by this disease.[1,2]

Nifurtimox and benznidazole (**Figure 1**) were developed over four decades ago, and they still remain the current treatment for American trypanosomiasis. These drugs are considered far from ideal, because they cause multiple side effects and have limited efficacy, especially in patients with chronic disease.[3] This makes necessary and urgent the development of new, more effective and less toxic drugs. Several molecules have been studied for their potential as trypanocidal.[4,5,6] Some coumarins have shown anti-*T. cruzi* properties,[7,8,9,10] and could become an alternative for the treatment of the disease.

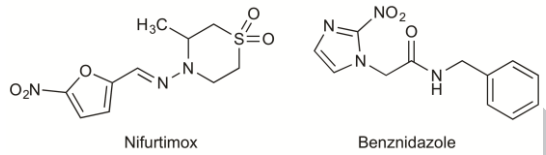

Figure 1. Chemical structures of the currently used antiparasitic drugs.

Coumarins are members of a huge family of compounds, structurally consisting in a benzene ring fused to a pyrone ring, with a carbonyl group at position 2.[11] The wide variety of biological properties of coumarins have drawn the attention of organic chemists. Both natural and synthetic coumarins own biological properties that depend on their chemical structure.[12] In particular, several compounds of this family present antioxidant capacity.[13,14,15,16]

Reactive oxygen species (ROS) are highly reactive molecules, which are principally generated by the cellular metabolism. These species induce oxidative damage in biomolecules, such as carbohydrates, proteins, lipids and nucleic acids. This deleterious effect on molecules has been related to ageing acceleration and other chronic diseases, such as neurodegenerative diseases, cancer and cardiovascular pathologies.[17] Antioxidant compounds, such as hydroxycoumarins, have been studied due to their ability to prevent neurodegenerative disorders. The potential mechanisms are related to the scavenging of free radicals and the delaying or prevention of biomolecules oxidation.[18]

Thuong *et al.* studied some coumarins with a catechol moiety, which showed interesting free radicals scavenging activity and lipid peroxidation inhibition. In addition, the α-pyrone ring in the coumarin framework proved to improve the inhibitory activity of oxidative reactions.[19] This is in accordance with the studies developed by our group on hydroxyl substituted 3-arylcoumarins.[18]

It has been shown that hydroxylated coumarins have both antioxidant and anti-*T. cruzi* activity.[8,20] Both properties might be considered necessary in the creation of new drugs with potential trypanocidal activity, since during the lifecycle of *T. cruzi* and the infection process ROS can be produced by parasite toxic secretions. Moreover, one of the mechanisms associated with trypanocidal activity of coumarins is the inhibition of GAPDH enzyme, related to oxidative stress generation.[21,22]

In this work a series of hydroxy-3-arylcoumarins (**Figure 2**) were synthesized and anti-*T. cruzi* activity and its relation to the antioxidant capacity were studied.

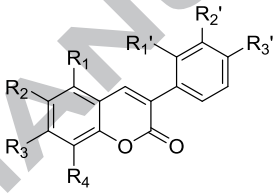

1: R_1, R_3, R_4, R_2', R_3' = H ; R_2, R_1' = OH
2: R_1, R_3, R_4, R_1', R_3' = H ; R_2, R_2' = OH
3: R_1, R_2, R_3, R_1', R_3' = H ; R_4, R_2' = OH
4: R_1, R_2, R_3, R_1' = H ; R_4, R_2', R_3' = OH
5: R_2, R_4, R_1', R_2', R_3' = H ; R_1, R_3 = OH
6: R_2, R_4, R_1', R_3' = H ; R_1, R_3, R_2' = OH
7: R_1, R_2, R_1', R_2', R_3' = H ; R_3, R_4 = OH
8: R_1, R_2, R_2', R_3' = H ; R_3, R_4, R_1' = OH
9: R_1, R_2, R_1', R_3' = H ; R_3, R_4, R_2' = OH
10: R_1, R_2 R_1' = H ; R_3, R_4, R_2', R_3' = OH

Figure 2. General structure of the studied hydroxy-3-arylcoumarins.

Results and Discussion

Chemistry

Compounds **1–10** were efficiently synthesized according to the synthetic strategy outlined in **Scheme 1**. The synthetic methodology involves a two-step synthetic route. The first step is a Perkin–Oglialoro condensation of the different commercially available hydroxybenzaldehydes and arylacetic acids, using potassium acetate (CH_3CO_2K) in acetic anhydride (Ac_2O), under reflux, for 16 h, to obtain the precursor acetoxy-3-arylcoumarins.[23] Acetylation of the hydroxyl groups and pyrone ring closure occur simultaneously. The second step is a hydrolysis of the obtained acetoxy derivatives, in the presence of aqueous HCl solution and MeOH, under reflux, for 3 h, to achieve the final substituted hydroxy-3-arylcoumarins (**1–10**). Structures of the synthesized compounds were established based on their spectral data (see the Experimental section).

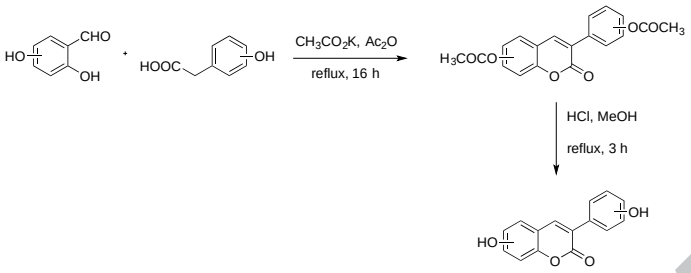

Scheme 1. Synthetic methodology to obtain the hydroxyl substituted 3-arylcoumarins.

Electrochemical study

Oxidation potential is a physicochemical parameter that determines the energy needed for a compound to give electrons. This parameter was obtained by means of the electrochemical technique, Cyclic Voltammetry (CV). Oxidation potentials have been related to the antioxidant capacity of polyphenols. This usually means that a low oxidation potential indicates a higher antioxidant capacity.[24,25] In this work, determinations of the oxidation potentials and the oxidation mechanisms of the hydroxy-3-arylcoumarins were performed in a polar aprotic medium.

To facilitate the discussion, the hydroxy-3-arylcoumarins were classified according to the position and number of the hydroxyl groups presented in the coumarin scaffold as: monohydroxylated derivatives (**1**-**3**), catechol derivatives (**4**, **7**-**10**) and resorcinol derivatives (**5** and **6**).

Among resorcinol derivatives, the CV of compound **5** shows a single signal for the oxidation cycle, and no signal in the reverse scan (reduction), indicating an irreversible oxidation in the experimental conditions (**Figure 3**). The same tendency was observed for compound **6**, which presents a similar CV profile and similar oxidation potential.

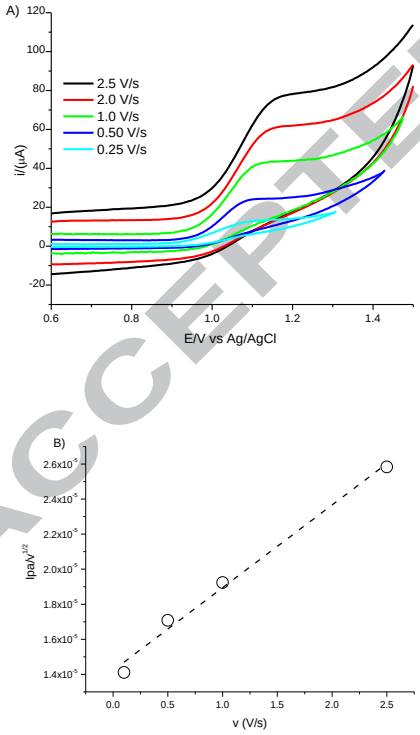

Figure 3. A) Cyclic voltammogram for 1 mmol/L of compound **5** for v= 0.1–2.5 mV/s; B) linear relationship between the ratio of Ipa /$v^{1/2}$ *versus* scan speed (v).

According to the reversibility criteria proposed by Nicholson and Shain and the absence of any cathodic peak (**Figure 3A**), the oxidation mechanism of these compounds could be associated to a chemical reaction followed by an irreversible electrochemical reaction.[26]

The anodic signal of the resorcinol derivatives is attributed to the oxidation of the corresponding resorcinol group to a *meta*-quinone through a *meta*-semiquinone radical (**Scheme 2**). This radical is not thermodynamically stable, and is rapidly reduced to the *meta*-quinone, and therefore no reduction peak is evident. The reduction potential of the hydroxyl groups in a coumarin ring is influenced by the position of this group.[27] This may justify the lower reactivity of the resorcinol moiety.

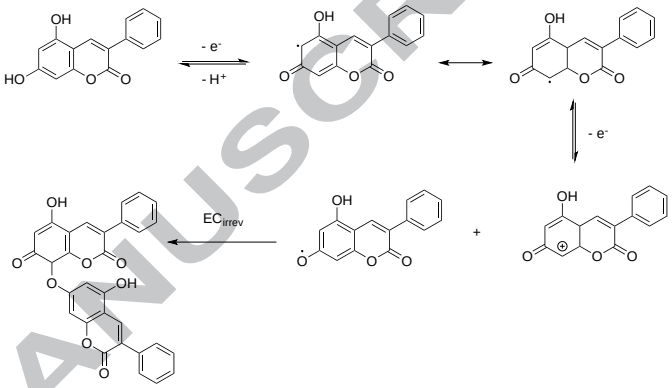

Scheme 2. Proposed electrochemical oxidation mechanism for compound **5**.

Monohydroxylated derivatives in the 3-aryl ring (**1**-**3**) also contain a second hydroxyl group in the coumarin core. Compound **2**, for example, has two hydroxyl groups in its structure: one at position 6 of the coumarin skeleton and another one at position 2' of the phenyl group. CV of compound **2** showed two anodic peaks, corresponding to the oxidation of both hydroxyl groups (**Figure 4**). The anodic peak at lower oxidation potential corresponds to the hydroxyl group at position 6 of the coumarin ring, regarding its relative position to the α-pyrone ring, thereby facilitating oxidation. The second anodic peak at a higher potential corresponds to the hydroxyl group present in the phenyl ring. A proposed oxidation mechanism is outlined in **Scheme 3**. Since these oxidation processes are faster than the scan rate, the process is observed as one wide peak. Due to the structural similarity between compound **2** and the compounds **1** and **3**, similar cyclic voltammograms were obtained. As well as for resorcinol derivatives, 3-aryl monohydroxylated derivatives **1**-**3** show irreversible oxidation, since there is no signal in the reverse scan (**Figure 4**).

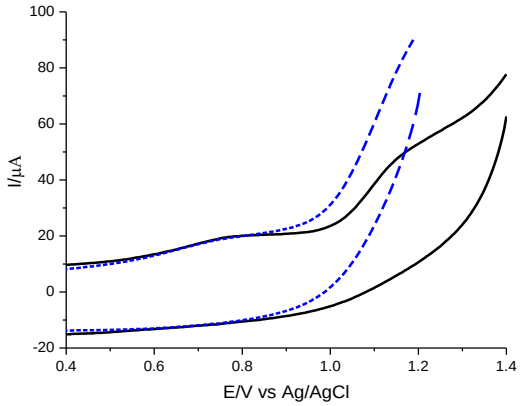

Figure 4. Cyclic voltammogram for 1 mmol/L of compound **2** (black) and **1** (dotted blue line), for v = 2.5 mV/s.

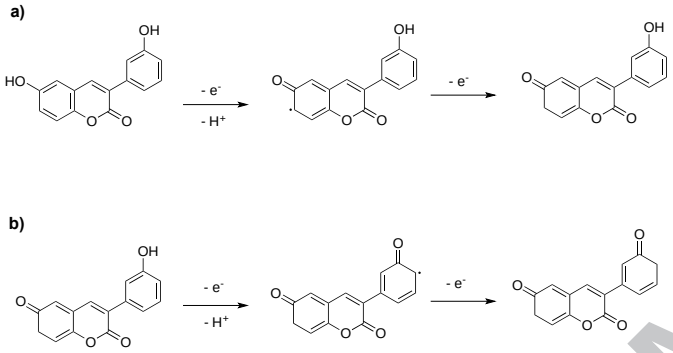

Scheme 3. Electrochemical oxidation mechanism proposed for compound **2**. a) oxidation mechanism of the hydroxyl group at position 6 of the coumarin ring; it corresponds to an anodic peak at lower potential. b) oxidation mechanism of the hydroxyl group at position 3' of the aromatic ring; it corresponds to an anodic peak at higher potential.

In the catechol derivatives (**4** and **7-10)**, compound **9** presents a quasi-reversible peak (**Figure 5A**). When two catechol groups were present in the molecule, such as for compound **10**, two anodic peaks were observed (**Figure 5B**).

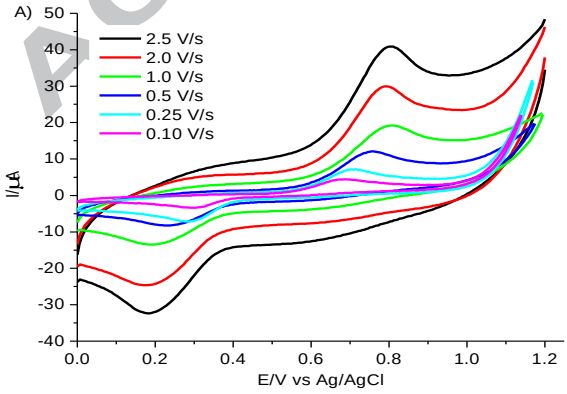

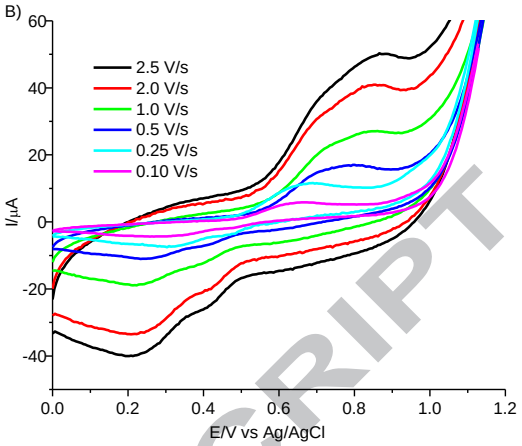

Figure 5. Cyclic voltammogram at v= 0.1–2.5 mV/s for 1 mmol/L of: A) compound **9** and B) compound **10**.

The anodic signal of the dihydroxycoumarins is attributed to the oxidation of the catechol group to the corresponding *ortho*-radical-semiquinone and then to the corresponding *ortho*-quinone (**Scheme 4**). In these cases, substitution in *ortho* position is a structural factor that should contribute to electron density favouring oxidative process, leading to the decrease in the oxidation potentials.[28]

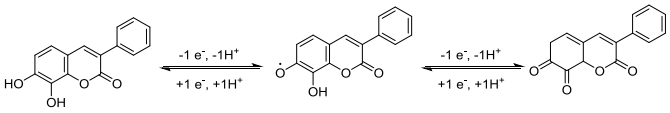

Scheme 4. Electrochemical oxidation mechanism proposed for compound **7**.

From the oxidation potentials point of view (**Table 1**) the antioxidant capacity of the compounds can be ranked as: **10** > **3** > **8** > **1** > **2** > **4** = **7** = **9** > **5**.

Derivatives with a catechol group in their structure presented an oxidation potential around 0.80 V, with exception of compound **10**, which presented two oxidation potential. From the catechol series, compound **8** shows the lowest anodic peak potential (Epa = 0.78 V) when compared to compounds **4**, **7** and **9**, which have similar anodic peak potentials (E_{pa} = 0.81 V in all three cases). Compound **10**, containing two catechol groups in its structure in both the aryl ring and the coumarin core, presents oxidation potentials at 0.64 and 0.79 V, and therefore showing the most promising antioxidant properties in the studied series.

Resorcinol derivatives (**5-6**) show higher anodic oxidation potentials compare to the catechol derivatives due to the *meta* position of the second hydroxyl group of the resorcinol derivatives, which does not provide electron density directly to the reaction centre (hydroxyl group at position 7). However, the

oxidation potentials of the catechol derivatives are lower since the formation of an *ortho*-semiquinone radical is stabilized by the presence of the hydroxyl group at *ortho* position with electron-donating properties to the reaction centre, thereby moving oxidation potentials to less positive values.

Characterization of radical species generated through electron spin resonance (ESR) spectroscopy

Electron spin resonance (ESR) is a spectroscopic technique for the detection of free radicals in the presence of a magnetic field, when irradiated with microwaves. For this reason, this technique has been employed for the detection and characterization of radicals generated by the oxidation of the tested hydroxylated coumarin derivatives.

The electrochemical oxidation of the hydroxylated coumarin derivatives was performed under the same conditions as for CV. Due to the short half-lives of the generated free radicals, it was necessary to use the spin-trapping methodology by using *N*-tert-butyl-α-phenylnitrone (PBN) as the spin-trap agent. The spin-trap is a diamagnetic compound that interacts with a free radical forming a paramagnetic spin-adduct. In this way, the half-life of a free radical increases and thus it makes possible its detection. PBN allows the detection of carbon- and oxygen-centred radicals. In the presence of PBN a six lines hyperfine pattern is obtained (**Figure 6**), with coupling constants a_N = 13.9 G and a_H = 2.3 G, indicating the trapping of a carbon-cantered free radical for compounds **1**, **2**, **5** and **6**.[29]

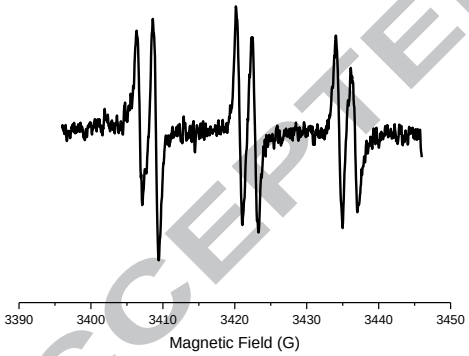

Figure 6. ESR spectra of compound **5**-PBN adduct in DMSO.

The free radical intermediates generated by the electrochemical oxidation of *ortho*-dihydroxycoumarin derivatives (catechol derivatives, compounds **4** and **7**-**10**) produced no signal structure employing the ESR technique. This is because the lifetimes of the generated radical species are very short to be measured experimentally, and the final products of oxidation are silent in ESR. For this reason, a zinc salt ($ZnCl_2$) was used, because complexation reaction between zinc (II) and the catechol moiety in these tested compounds brings stability to the *ortho*-semiquinone radical. As a result, the radical can be experimentally measured at room temperature.[30]

For the compounds mentioned above, the electroactive group is the catechol moiety and therefore the intermediate could be the *ortho*-semiquinone radical. This was confirmed by the simulation of the electrochemical oxidation of the coumarin derivative **10** by EPR-WinSIM (**Figure 7**). Compound **10** presented a symmetrical two-line spectrum, which is interpreted in terms of the formation of a semiquinone radical whose relocation is through the benzene ring of the coumarin skeleton.

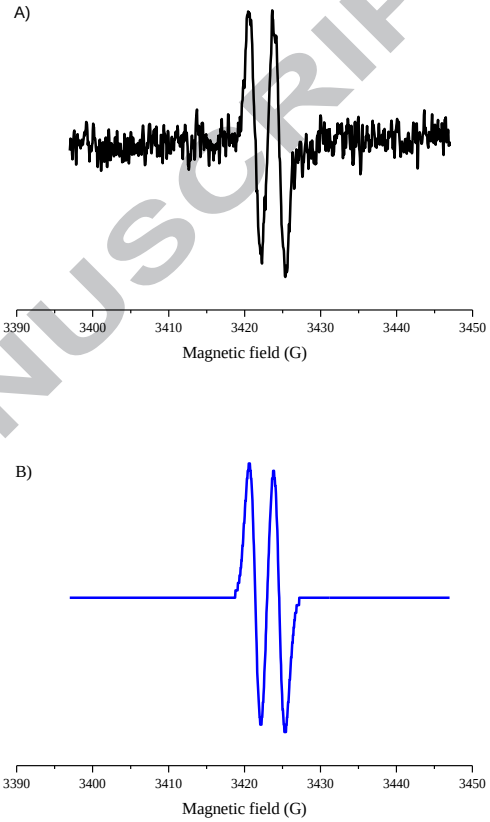

Figure 7. A) ESR experimental spectrum corresponding to the radical derived from the electrochemical oxidation stabilized derivative compound **10** Zn^{+2}. B) ESR simulated spectrum of compound **10** by the EPR-WinSim program.

Compound **7** has a hyperfine pattern of two lines with a hyperfine-coupling constant of 3.14 G, showing the same behaviour as compound **10**.

According to the analysis of the ESR spectrum of catechol derivatives **4** and **7**-**10**, it could be possible to confirm that the oxidation of the catechol moiety in these compounds goes through the formation of an *ortho*-semiquinonic radical intermediate. According to this, we can confirm the proposed electrochemical oxidation mechanism (**Scheme 4**) for these compounds.

Study of the reactivity towards the hydroxyl radical

Reactivity against the hydroxyl radical (OH•) was studied by means of the spin-trapping methodology, which is based on the competitive reactions between the coumarin derivative and the

spin-trap (DMPO) for the OH•. The OH• was generated *in situ* by UV-photolysis of hydrogen peroxide. A hyperfine pattern of four lines with intensities in the ratio of 1:2:2:1 was obtained. This spectrum is characteristic of the spin-adduct [DMPO-OH].[31] Scavenging of the OH• was calculated by adding a constant concentration of the corresponding derivative and measuring the decrease percentage in the integration of the signals regarding to the control solution, which do not contain the studied compound.

In **Table 1** it is shown that compounds **1**, **3**, **4** and **6**-**8** have the no reactivity against OH•. On the other hand, compounds **2** and **5** proved to be display an ability to completely scavenge radicals. As a consequence of these results, there is not a direct relation between the number of hydroxyl groups in the coumarin skeleton and the antioxidant capacity. Compound **2** (presenting only one hydroxyl group on the coumarin core at position 6) completely scavenge the OH•. This could be explained due to the relative position of the hydroxyl group to the coumarin core, favouring the radical stabilization.

The possible structural differences between the catechol derivatives **9** and **10** and the resorcinol derivative **5** are mainly due to the potential formation of an intramolecular hydrogen bond between the hydroxyl group at the position 8 and the oxygen of the pyrone ring. While this interaction may take place in compounds **9** and **10**, that does not occur in the resorcinol derivatives.

Table 1. Results obtained in antioxidant homogeneous assays (ORAC-FL, oxidation potential and scavenging of OH•).

Compounds	Oxidation potential (V)		OH• Scavenging (%)	ORAC-FL index
	Epa_1	Epa_2		
1	0.79	--	--	5.30 ± 0.29
2	0.80	1.17	100	5.47 ± 0.31
3	0.74	--	--	3.12 ± 0.50
4	0.81	--	--	4.59 ± 0.02
5	1.16	--	100	1.81 ± 0.05
6	--	--	--	1.95 ± 0.14
7	0.81	--	--	1.11 ± 0.04
8	0.78	--	--	2.23 ± 0.19
9	0.81	--	26.09	2.95 ± 0.50
10	0.64	0.79	24.29	5.38 ± 0.50
Trolox*	--	--	31	**1.0** ± 0.2

-- parameter not observed

***** Data obtained from references [32] and [33].

Determination of antioxidant capacity by ORAC-FL assay

All the studied compounds showed higher antioxidant capacity than the standard compound, trolox. Regarding to the ORAC-FL assay, the compound showing the best ORAC-FL index is compound **2** (**Figure 8**). Based on the ORAC-FL index, the order from the highest to the lowest scavenging activity against the peroxyl radicals in this series is: **2** > **10** > **1** > **4** > **3** > **9** > **8** > **6** > **5** > **7**.

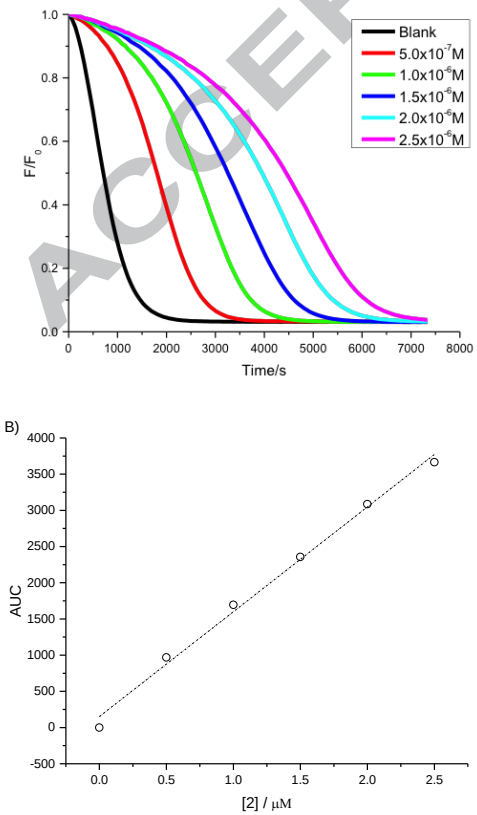

Figure 8. A) ORAC-FL profile for compound **2**; B) AUC as a function of the concentration for compound **2**.

Despite monohydroxylated derivatives **1**-**3** only present one hydroxyl group in the coumarin core and another hydroxyl group in the 3-phenyl ring, compounds **1** and **2** displayed the highest ORAC-FL indexes of all the studied compounds. This might be attributed to the presence of the hydroxyl group at position 6, which is located in the opposite position to the cyclic ester. This makes possible an easy transfer of a hydrogen atom to the peroxyl radical.

On the other hand, the lowest ORAC-FL index was presented by compound **7**. A possible explanation is that the hydroxyl group at position 8 forms a hydrogen bond with the oxygen in the pyrone ring, thus reducing their ability to transfer to peroxyl radicals. Compounds **7**-**9** are structurally similar, as they both contain a catechol group at 7,8-positions of the coumarin ring, and varies in the presence and/or position of the hydroxyl substituent on the 3-phenyl ring. In general, the presence of a catechol moiety in the structure increases the antioxidant properties in a polyphenolic compound due to the stability of the *ortho*-semiquinone radical.[34] However, these compounds have low ORAC-FL values. This has been attributed to the formation of an intramolecular hydrogen bond between the hydroxyl group at position 8 and the oxygen of the α-pyrone ring affecting the ability to donate the hydrogen atom. Therefore, their antioxidant capacity is reduced. However, when comparing the catechol derivatives, we observed that the presence of the hydroxyl group in the 3-phenyl ring (compounds **4**, **8**-**10**) increases the antioxidant capacity in at least double comparing to compound **7**. Position and number of the hydroxyl groups in the 3-phenyl ring plays an important role in the antioxidant capacity. Compound **9** (3'-OH) presented a slightly

significant higher activity than compound **8** (2'-OH), and compound **10** (2',3'-OH) showed the best ORAC-FL index of the catechol series.

Compounds **4** and **10**, with ORAC-FL values of 4.59 and 5.38, respectively, presented the highest antioxidant capacity in the catechol series due to the presence of a catechol moiety in the 3-phenyl ring. Compound **10** increases the antioxidant capacity in 5-fold comparing to compound **7**. Compound **4** has not significant difference with the ORAC-FL index of the 8-hydroxy-3-arylcoumarin (ORAC-FL = 5.7) previously described by our group.[18]

Resorcinol derivatives **5** and **6** showed low ORAC-FL values due to the *meta* position of the hydroxyl groups. This position performs an electro-withdrawing effect affecting the ability to donate the hydrogen atom, resulting in low ORAC-FL values.[35]

According to the obtained results, there is no clear relationship between the number of hydroxyl groups and the ORAC-FL values. However, regarding the results herein analyzed the most beneficial positions of the hydroxyl groups are on the 3-arylcoumarin frame.

Determination of the cytotoxic activity against *T. cruzi* (Dm28c clone) epimastigotes forms

The activity of the coumarin derivatives were evaluated in mammalian cells as hosts for parasites in order to assess the cytotoxicity of these compounds in RAW 264.7 murine cells (macrophages from blood). A preliminary screening based on the cell viability was carried out using 100 µM concentrations and comparing the results to a control (**Figure 9**).

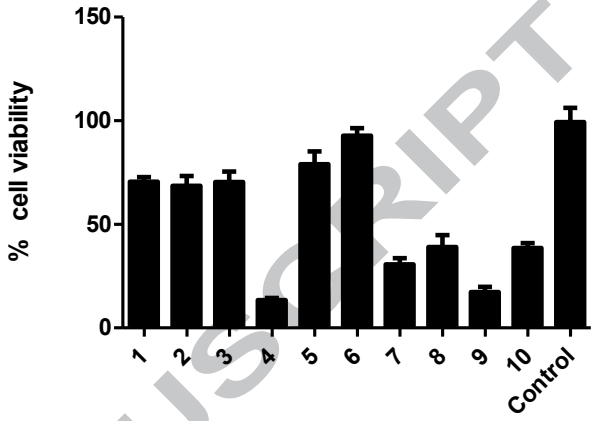

Figure 9. Cell viability of hydroxy-3-arylcoumarins on RAW 264.7 cells. The results correspond to the mean ± SD of three independent experiments.

Based on the screening, the IC_{50} values were calculated in RAW 264.7 macrophages. Results are summarized in **Table 2**.

Table 2. *In vitro* cytotoxicity in murine RAW 264.7 macrophages (IC_{50}) and trypanocidal activity in epimastigote.

Compounds	IC_{50} (µM)		
	RAW 264.7	**Epimastigotes**	**SI***
1	> 100 **	> 100 **	-
2	> 100 **	> 100 **	-
3	> 100 **	> 100 **	-
4	115.30 ± 0.99	84.28 ± 7.38	1.37
5	> 100 **	6.15 ± 5.01	> 16.26
6	> 100 **	> 100 **	-
7	26.10 ± 4.19	8.90 ± 5.25	2.93
8	68.85 ± 0.65	1.31 ± 2.03	52.56
9	397.60 ± 29.56	28.55 ± 5.07	13.93
10	97.48 ± 7.95	46.99 ± 3.41	2.07
Nifurtimox	263.44	17.4 ± 1.3	15.14

* Selectivity Index IC_{50} macrophages RAW 264.7/IC_{50} epimastigotes clone Dm28c

** 100µM was the highest tested concentration. At higher concentrations, the compounds precipitate and data could not be attained.

Based on the IC_{50} values, exactly half of the studied derivatives showed low cytotoxicity on RAW 264.7 macrophages. Compound **7** showed the highest cytotoxicity against the evaluated mammalian cells (IC_{50} = 26.10 ± 4.19 µM).

The determination of viability of epimastigote of *T. cruzi* Dm28c, was performed using concentrations 100 and 10 µM of coumarin derivatives (**Figure 10**).

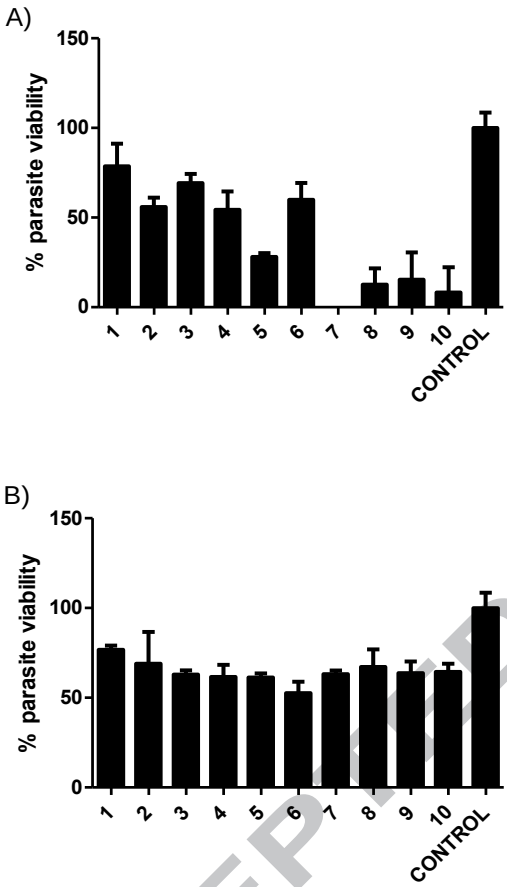

Figure 10. Parasite viability of the studied 3-arylcoumarins on epimastigotes of *T. cruzi* (clone Dm28c) (A) 100 µM and (B) 10 µM. The results correspond to the mean ± SD of three independent experiments. The results are normalized in relation to the control, which represents 100% of viability.

In general, it is observed that the catechol moiety at 7,8-positions of the coumarin skeleton improved the trypanocidal activity in the epimastigote stage. On the other hand, the derivatives with one hydroxyl group on the coumarin moiety showed low activity in the epimastigote stage.

The IC_{50} values against the epimastigote form of the *T. cruzi* were calculated, as well as the selectivity index (SI, **Table 2**). Compounds **5**, **8** and **9** presented the best selectivity index ranging from 13.93 to 52.56, being compound **8** the most selective of the series (3.5 times more selective than Nifurtimox).

The viability of the epimastigotes form of *T. cruzi* was correlated to the antioxidant capacity of hydroxy-3-arylcoumarins, in order to obtain information about the possible mechanism of trypanocidal action.

It can be seen in **Figure 11**, that the hydroxy-3-arylcoumarins with greater trypanocidal activity (compounds **8** > **5** > **7**) have lower antioxidant capacity (ORAC-FL index similar between them) than the others. In contrast, the compounds with lower trypanocidal activity have better antioxidant capacity. Overall, mono-hydroxylated coumarins in the 3-phenyl ring proved to display lower activities on epimastigotes form of the parasite.

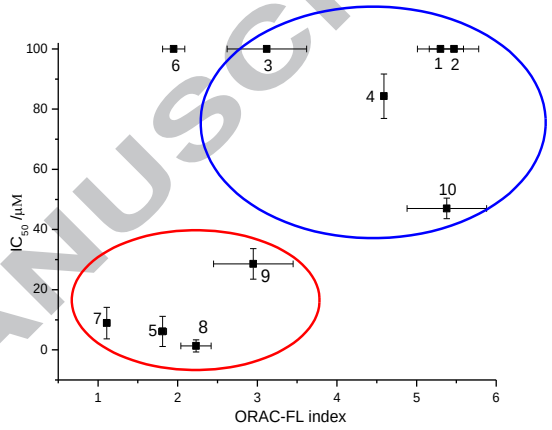

Figure 11. Correlation between antioxidant capacity and viability of the epimastigote form of *T. cruzi* in the presence of hydroxy-3-arylcoumarins. Red circle – compounds with major trypanocidal activity and minor antioxidant capacity. Blue circle – compounds with minor trypanocidal activity and major antioxidant capacity.

According on the above, it can be stated that there is no direct relationship between the properties in compounds in study, indicating two independent action mechanisms.

In order to obtain information about the possible mechanism of action via oxidative stress, the ESR spectrum was recorded in parasitical medium.

Detection of free radicals generated by coumarin derivatives in a parasitic medium (epimastigote form of *T. cruzi*) by means of the spin-trapping methodology assisted by ESR

To perform the free radical detection in a microsomal parasitic medium, an ESR technique was employed. A solution of DMSO was used as a control, without detecting the generation radical species.

In this assay, the most active compounds were compounds **5**, **7** and **8**, at a concentration of 5 mM (**Figure 12**). All these compounds generated the same spectral pattern after ten minutes of incubation. The strong intensity of the observed signals is consistent with the trapping of a carbon-centred radical, which might be the coumarin derivative radical (aH ~ 20.06 G and aN ~ 15.76 G).

Because the control solution did not show any signal, it may be deduced that the DMPO does not break down immediately and that no free radical is being trapped by the DMPO. Moreover, it is possible to observe the quartet splitting pattern (aN~aH~14.87 G) due to the DMPO-OH radical adduct. This evidences the *in situ* formation of the OH• by the incubation of coumarin derivatives. Subsequently, this adduct can undergo an oxidative process, thereby forming a paramagnetic compound (DMPOX, 5,5-dimethyl-2-oxo-pyrrolin-1-oxyl),[36] which is observed in the spectrum as a triplet (aN ~ 15.46 G). These results may indicate that mechanism of action of these hydroxylated coumarins could go through the generation of ROS (see **Figure 13**), i.e. a possible *via* would be the oxidative stress. These results are related to ones described by Aguilera-Venegas *et al*.,6 in which the generation of oxidative stress is evident, possibly with a mechanism associated to the generation of mitochondrial alterations in the parasite.

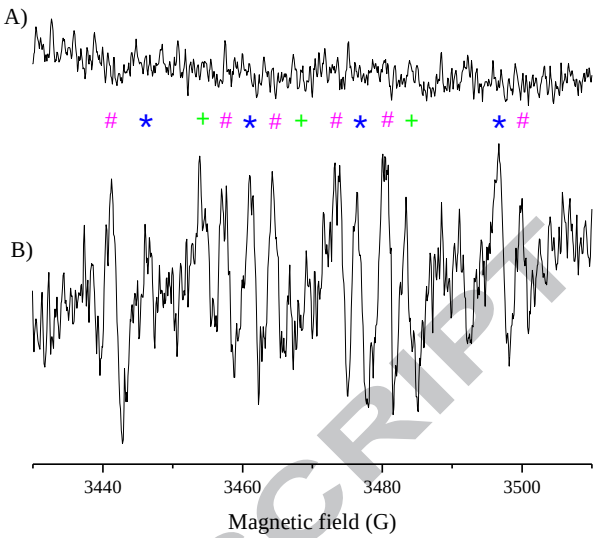

Figure 12. Experimental spectrum for spin-adduct generated in microsomes *T. cruzi* (strain Dm28c) at room temperature: a) Spectrum of the control sample (DMSO); b) Spectrum recorded with the microsomal fraction incubated with compound **5** and DMPO. It has been marked (*) the corresponding hyperfine pattern for the spin-adduct DMPO-OH. The hashtag (#) indicates the adduct between a carbon-centred radical and DMPO, and (+) indicate the DMPOX adduct.

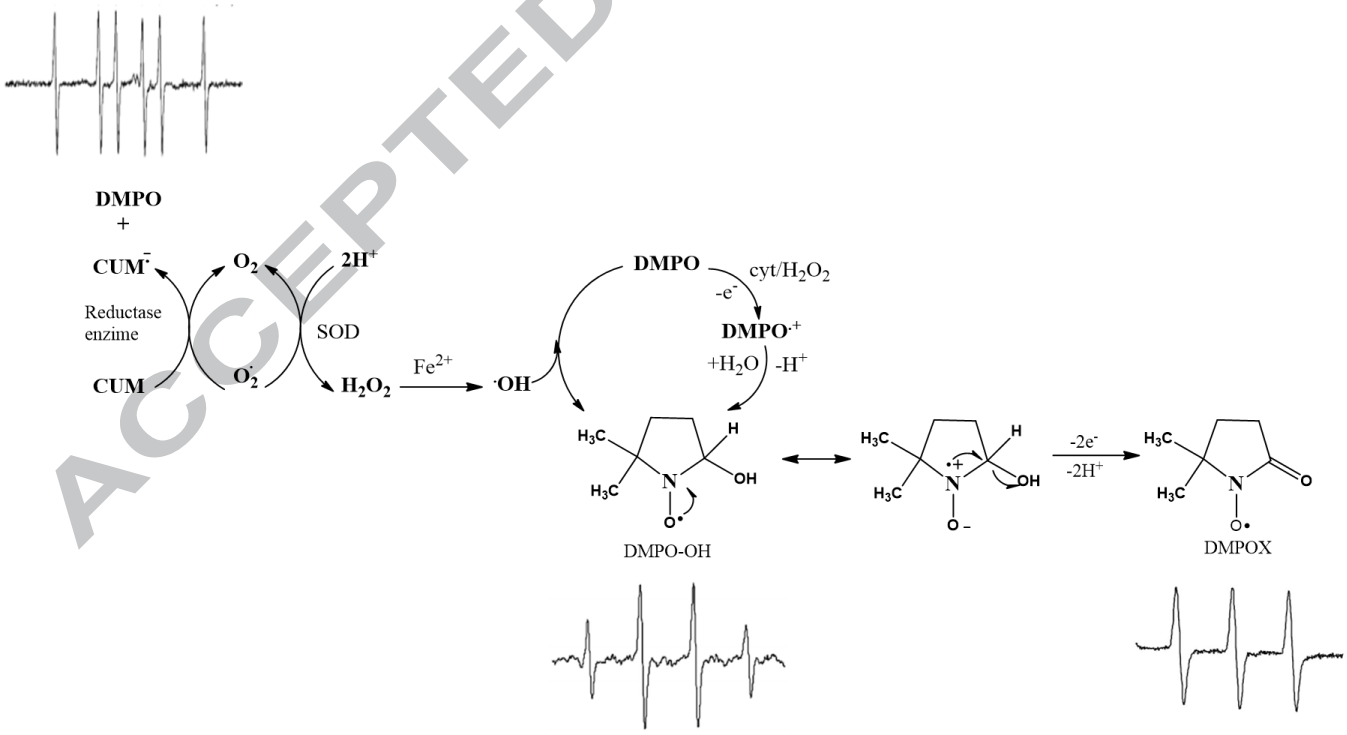

Figure 13. Mechanism of action proposed of hydroxy-3-arylcoumarins against epimastigotes of *T. cruzi*, generation of metabolites and their interaction with the spin trap DMPO. Spectra of ESR of DMPO-CUM (carbon centred, sextet of intensity 1:1:1:1:1:1), DMPO-OH (quartet of intensity 1:2:2:1) and DMPOX (triplet of intensity 1:1:1).

Determination of activity gainst trypomastigote form of *T. cruzi* (Dm28c clone).

The three most active compounds against epimastigote form of the parasite, were selected to be studied on the trypomastigote form.

The compounds were evaluated at 20 and 100 µM (**Figure 14**) against the trypomastigote form. Since only compound **8** showed a significant activity against the trypomastigote form, its IC_{50} value was the only one determined (**Table 3**). Compound **8** resulted to be more active against the epimastigote form (IC_{50} = 1.31 µM) than against the trypomastigote one (IC_{50} = 39.73 µM). However, in the epimastigote stage, compound **8** was more than 10 times more active than Nifurtimox. The selectivity of compound **8** between the macrophages (RAW 246.7 cells) and the parasites (epimastigote form) was higher (SI = 52.56) than Nifurtimox (SI = 15.14), but the window between the IC_{50} in both cell lines was narrower than for Nifurtimox.

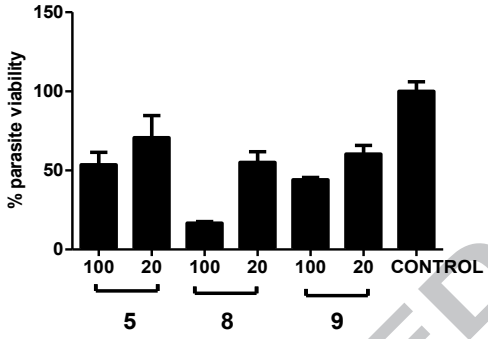

Figure 14. Parasite viability of compounds **5**, **8** and **9** on *T. cruzi* trypomastigote form (clone Dm28c) to the concentration of 20 and 100 µM. The results correspond to the mean ± SD of three independent experiments. The results were normalized for the control, representing 100% viability.

Table 3. *In vitro* cytotoxicity of compound **8** (against epimastigote and trypomastigote stages of *T. cruzi*).

***T. cruzi* stage**	**Compound 8**		**Nifurtimox**	
	IC_{50} (µM)	**SI***	**IC_{50} (µM)**	**SI***
Epimastigote	1.31 ± 2.03	52.56	17.40 ± 1.30	15.14
Trypomastigote	39.73 ± 2.80	1.73	10.00 ± 0.40	26.34

* Selectivity Index = IC_{50} macrophages RAW 264.7/IC_{50} *T. cruzi* (parasite).

From the results for the trypomastigote stage, we can say that derivatives with a catechol moiety at 7,8-positions in the coumarin core showed significant activity. This activity improved when a hydroxyl group was added to position 2' of the 3-phenyl ring. These results give some interesting information about the structural properties and the trypanocidal activity, based on the compound **8** structure, for the design of new hydroxy-3-arylcoumarins.

3. Conclusions

Electrochemical studies indicated that coumarins bearing resorcinol groups at the 3-phenyl ring and a hydroxyl group in the coumarin core display an irreversible oxidation process. Coumarins with catechol groups have a quasi-reversible oxidation process. The oxidation potentials of these coumarins proved to be lower than the compounds with resorcinol groups in their structures. This was detected and characterized by ESR assays, confirming the mechanism proposed by CV. For the case of radical species with a short half-life, it was detected by a spin trapping technique. The antioxidant reactivity towards OH• was evaluated by the spin trapping methodology and showed that there is no correlation between the number of hydroxyl groups in the molecule and its reactivity. All the studied coumarins were more active than trolox in the ORAC-FL assay. Coumarins having a hydroxyl group at position 6 and a catechol group in the 3-aryl ring showed the best antioxidant capacity of the studied series. Most of the evaluated compounds showed low cytotoxicity against RAW 264.7 macrophages, particularly those compounds that showed higher antioxidant capacity. In the *in vitro* study of the trypanocidal ability, compound **8** was active against both epimastigote and trypomastigote forms of the parasite, and up to 13 times more active than Nifurtimox against the epimastigote form. The presence of a catechol group at 7,8-positions of the coumarin core proved to be critical for the trypanocidal activity, as observed for compounds **8** and **9**. The generation of radical species in the epimastigote form after incubation with coumarins suggests that the cytotoxicity mechanisms could occur by generating oxidative stress to the parasite. Rational design using compound **8** as lead compound would allow the generation of new series of compounds displaying important trypanocidal properties.

4. Experimental section

Synthetic procedures

The starting materials and reagents were obtained from commercial suppliers (Sigma-Aldrich) and were used without further purification. Melting points (Mp) are uncorrected and were determined using a Reichert Kofler Thermopan or in capillary tubes in a Büchi 510 apparatus. ^{1}H NMR (250 MHz) and ^{13}C NMR (75.5 MHz) spectra were recorded using a Bruker AMX spectrometer using $CDCl_3$ or DMSO-d_6 as solvent. Chemical shifts (δ) are expressed in parts per million (ppm) using TMS as an internal standard. Coupling constants J are expressed in Hertz (Hz). Spin multiplicities are given as s (singlet), d (doublet), dd (doublet of doublets) and m (multiplet). Mass spectrometry was carried out using a Hewlett-Packard 5988 A spectrometer. Elemental analyses were performed by using a Perkin-Elmer 240B microanalyzer and the results are within ±0.4% of calculated values in all cases. The analytical results document ≥98% purity for all compounds. Flash chromatography

(FC) was performed on silica gel (Merck 60, 230–400 mesh); analytical TLC was performed on precoated silica gel plates (Merck 60 F254). Organic solutions were dried over anhydrous sodium sulfate. Concentration and evaporation of the solvent after reaction or extraction were carried out on a rotary evaporator (Büchi Rotavapor) operating under reduced pressure.

General procedure for the synthesis of acetoxy-3-arylcoumarins. The compounds were synthesized under anhydrous conditions, using a material previously dried at 60 °C for at least 12 h and at 300 °C for a few minutes immediately before use. A solution containing anhydrous CH_3CO_2K (2.94 mmol), the corresponding arylacetic acid (1.67 mmol) and the corresponding hydroxysalicylaldehyde (1.67 mmol), in Ac_2O (1.2 mL), was refluxed for 16 h. The reaction mixture was cooled, neutralized with 10% aqueous $NaHCO_3$, and extracted with EtOAc (3 x 30 mL). The organic layers were combined, washed with water, dried over anhydrous Na_2SO_4 and the solvent was evaporated under reduced pressure. The product was purified by recrystallization in EtOH and dried in vacuum to afford the desired compound.

General procedure for the synthesis of hydroxy-3-arylcoumarins (1–10). Compounds **1**–**10** were obtained by hydrolysis of their acetoxylated counterparts, respectively. The appropriate acetoxylated coumarin, mixed with 2N aqueous HCl and MeOH, was refluxed for 3 h. The resulting reaction mixture was cooled in an ice-bath and the reaction product and the obtained solid was filtered, washed with cold distilled water, and dried under vacuum, to afford the desired compounds (**1**–**10**).

6-Hydroxy-3-(2'-hydroxyphenyl)coumarin (1). Mp. 226-227 °C. Yield 87 %. ^{1}H NMR (250 MHz, DMSO-d_6) δ: 6.84-6.90 (m, 2H, H-3', H-5'), 7.01-7.06 (m, 2H, H-7, H-4'), 7.24-7.43 (m, 3H, H-5, H-8, H-6'), 7.91 (s, 1H, H-4), 9.54 (1H, OH), 9.70 (1H, OH). ^{13}C NMR (75.5 MHz, DMSO-d_6) δ: 115.6, 118.1, 118.8, 119.3, 120.7, 124.7, 125.0, 126.8, 129.4, 136.1, 141.0, 141.7, 144.4, 157.2, 171.8. MS *m/z*: 254 ([M+1]$^+$, 100 %). Ana. Elem. Calc. for $C_{15}H_{10}O_4$: C, 70.86; H, 3.96. Found: C, 70.84; H, 3.93.

8-Hydroxy-3-(3'-hydroxyphenyl)coumarin (3). Mp. 245-246 °C. Yield 89 %. ^{1}H NMR (250 MHz, DMSO-d_6) δ: 6.83-6.89 (m, 1H, H-4'), 7.12-7.29 (m, 3H, H-2', H-5', H-6'), 7.14-7.25 (m, 3H, H-5, H-6, H-7), 7.91 (s, 1H, H-4), 9.63 (1H, OH), 9.89 (1H, OH). ^{13}C NMR (75.5 MHz, DMSO-d_6) δ: 113.9, 117.8, 118.2, 119.7, 120.1, 123.6, 125.3, 127.2, 129.7, 135.4, 140.7, 141.9, 145.9, 158.1, 169.3. MS *m/z*: 254 ([M+1]$^+$, 100 %). Ana. Elem. Calc. for $C_{15}H_{10}O_4$: C, 70.86; H, 3.96. Found: C, 70.87; H, 3.95.

5,7-Dihydroxy-3-(3'-hydroxyphenyl)coumarin (6). Mp. 276-277 °C. Yield 93 %. ^{1}H NMR (250 MHz, DMSO-d_6) δ: 6.21-6.27 (m, 2H, H-6, H-8), 6.71-6.79 (m, 1H, H-4'), 7.02-7.23 (m, 3H, H-2', H-5', H-6'), 8.00 (s, 1H, H-4), 9.51 (s, 1H, OH), 10.38 (s, 1H, OH), 10.75 (s, 1H, OH). ^{13}C NMR (75.5 MHz, DMSO-d_6) δ: 93.8, 102.4, 113.2, 115.2, 119.8, 120.3, 120.9, 129.4, 131.2, 136.7, 138.0, 156.3, 157.2, 162.2, 172.1. MS *m/z*: 270 ([M+1]$^+$, 100 %). Ana. Elem. Calc. for $C_{15}H_{10}O_5$: C, 66.67; H, 3.73;. Found: C, 66.65; H, 3.70.

7,8-Dihydroxy-3-(2'-hydroxyphenyl)coumarin (8). Mp. 215-216 °C. Yield 93 %. ^{1}H NMR (250 MHz, DMSO-d_6) δ: 6.84-6.90 (m, 2H, H-3', H-5'), 7.01-7.06 (m, 1H, H-4'), 7.12-7.34 (m, 3H, H-5, H-6, H-6'), 7.91 (s, 1H, H-4), 9.45 (s, 1H, OH), 10.13 (s, 1H, OH), 10.36 (s, 1H, OH). ^{13}C NMR (75.5 MHz, DMSO-d_6) δ: 112.7, 115.7, 119.0, 121.2, 122.8, 123.8, 129.7, 131.0, 132.0, 133.2, 136.5, 143.3, 149.2, 155.1, 160.1. MS *m/z*: 270 ([M+1]$^+$, 100 %). Ana. Elem. Calc. for $C_{15}H_{10}O_5$: C, 66.67; H, 3.73;. Found: C, 66.67; H, 3.71.

7,8-Dihydroxy-3-(3'-hydroxyphenyl)coumarin (9). Mp. 240-241 °C. Yield 88 %. ^{1}H NMR (250 MHz, DMSO-d_6) δ: 6.74-6.83 (m, 2H, H-4', H-6'), 7.07-7.13 (m, 3H, H-5, H-6, H-2'), 7.18-7.24 (t, 1H, H-5'), 8.06 (s, 1H, H-4), 9.51 (s, 1H, OH), 9.93 (s, 1H, OH), 10.28 (s, 1H, OH). ^{13}C NMR (75.5 MHz, DMSO-d_6) δ: 112.9, 115.2, 115.4, 119.1, 119.4, 122.1, 129.3, 131.9, 136.5, 141.6, 149.7, 157.2, 160.1, 171.4, 180.9. MS *m/z*: 270 ([M+1]$^+$, 100 %). Ana. Elem. Calc. for $C_{15}H_{10}O_5$: C, 66.67; H, 3.73;. Found: C, 66.69; H, 3.75.

Evaluation of ORAC-FL activity

The assays were carried out in a Synergy HT Multi-Detection Microplate Reader, from BioTek Instruments, Inc. (Winooski, USA), using polystyrene 96-well plate, purchased from Nunc, Denmark. Fluorescence was measured from the top, at an excitation wavelength of 485/20 nm and an emission at 528/20 nm. The plate reader was controlled by Gen5 software. The reaction was performed at 37 °C in 75 mM of phosphate buffer solution (pH = 7.4), to obtain a final volume of 200 µL. Fluorescein (final concentration, 40 nM) and stocks solutions of compounds were prepared in methanol because of their low solubility in buffer at high concentrations. A set of compounds solutions, in a range of final concentrations between 0.5 and 2.5 µM, was placed in each well of a 96-well plate. These concentrations allowed the separation of the fluorescence decay curves. The mixture was pre-incubated for 15 min at 37°C before the addition of the 2,2′-azobis(2-methylpropionamidine)dihydrochloride (AAPH) solution (final concentration, 18 mM). The microplate was immediately placed in the reader and automatically shaked prior to each reading. The fluorescence was recorded every 1 min for 120 min. A control assay with fluorescein, AAPH, and methanol (instead of the antioxidant solution) was performed for each assay.[37] Trolox was employed as standard antioxidant, in a final concentration range of 0.5–2.5 µM. The inhibition capacity was expressed as ORAC-FL values and is quantified by integration of the area under the curve (AUC_{NET}). All reaction mixtures were prepared in triplicate and at least three independent assays were performed for each sample. The area under the fluorescence decay curve (AUC) was calculated integrating the decay of the fluorescence where F_0 is the initial fluorescence read at 0 min and F is the fluorescence read at time. The net AUC corresponding to the sample was calculated by subtracting the AUC corresponding to the blank.

Data processing was performed using Origin Pro 8 SR2 (Origin Lab Corporation, USA).). The ORAC-FL indexes were calculated according to the following equation (1):

ORAC-FL index=

$[(AUC_{AH}–AUC_{control})/(AUC_{trolox}–AUC_{control})$ x [Trolox]/[AH]

Evaluation of redox properties by CV

CV measurements were performed in a Metrohm 693VA instrument with a 694VA stand convertor and a 693VA processor, at room temperature, using a three-electrode cell. A glassy carbon electrode presenting an area of 0.03 cm^2 was used as the working electrode. The electrode surface was polished with alumina powder (particle sizes, 0.3 and 0.05 mm) before use and after each measurement. Platinum wire was the auxiliary electrode and silver/silver chloride (Ag/AgCl, 3 M KCl) of Metrohm Company was used as a reference electrode. The CV experiments were carried out in DMSO, with 0.1 M of tetrabutylammonium perchlorate (TBAP) as supporting electrolyte and 1 mM of each coumarin derivative. Potential sweeps were executed between 0.0 and + 1.4 V, and 0.1–2.5 V/s.

Monitoring of electrochemically generated radicals by ESR

ESR spectra were recorded in the X band (9.85 GHz) using a Bruker ECS106 spectrometer with a rectangular cavity and 50-kHz field modulation. The hyperfine splitting constants were estimated to be accurate within 0.05 G. The phenoxyl radicals were generated by an *in situ* electrolytic oxidation process under the same experimental conditions as those of CV, in DMSO with 0.1 M of TBAP. The oxidation potentials were acquired from CV. Every spectrum was obtained after 50 scans. For catechol systems, radicals were stabilized by adding 0.01 M of zinc chloride. For monohydroxylated and resorcinol systems, radicals were trapped by adding 200 mM of *N*-*tert*-butyl-α-phenylnitrone (PBN). ESR spectra were simulated using the program EPR-WinSIM Version 0.98.

Reactivity against the hydroxyl radical (OH•)

The spin trapping technique involves short half-life free radicals with a diamagnetic molecule (spin trap), driving to the formation of a more stable free radical (spin-adduct) than the original radical, this new species can be detected by ESR technique.

In this case the OH• was studied and the spin trap DMPO (5,5-dimethyl-1-pyrroline) was employed. The OH• was generated by means of photolysis with ultraviolet light. This solution was prepared with 100 µL of 30% H_2O_2, 50 µL of DMPO solution (200 mM) and 50 µL of a 1 mM antioxidant solution. This solution was placed in a quartz EPR cell and after 2 minutes of UV-radiation the spectrum was taken.

ESR spectra were recorded in the X band (9.7 GHz) using a Bruker ECS 106 spectrometer with a rectangular cavity and 50-kHz field modulation, equipped with a high-sensitivity resonator at room temperature. Spectrometer conditions were: microwave frequency 9.81 GHz; microwave power 20 mW; modulation amplitude 0.91 G; receiver gain 59 dB; time constant 81.92 msec; and conversion time 40.96 msec. The results are given as a percentage of scavenging of the OH• in comparison to the control solution (which does not contain any antioxidant).

Evaluation of the cytotoxic and trypanocidal activity

Cytotoxicity assay

The effect of drug treatments on RAW 264.7 cells was evaluated through the tetrazolium dye (MTT; 3[4,5-dimethylthiazol-2-yl]-2,5-diphenyltetrazolium bromide) assay as a viability test.[38] Briefly, 10 µl of 5 mg/mL MTT plus 0.22 mg/mL phenazine metosulfate (electron carrier), were added to each well containing RAW 264.7 cell culture in 100 µL RPMI 1640 without phenol red. Compounds under study, dissolved in DMSO, were added to the culture media at the concentrations demonstrated in the figures and tables. DMSO final concentration was less than 0.25% v/v. After incubation for 4 h at 37 °C, the generated water-insoluble formazan dye was dissolved by the addition of 100 µL of 10% w/v sodium dodecyl sulphate (SDS) in 0.01 M HCl. The plates were further incubated overnight at 37 °C, and optical density of the wells was determined using a microplate reader (Asys Expert Plus©, Asys Hitach, Austria) at 570 nm. Under these conditions, the optical density is directly proportional to the viable cell number in each well. All experiments were performed at least three times and data reported as means and their standard deviations from triplicate cultures. Results are reported as the percentage of non-viable RAW 264.7 cells regarding the control (cells in culture medium).

Determination of trypanocidal activity

Epimastigote stage viability study

Trypanocidal activity was evaluated against the *T. cruzi* epimastigote stage (clone Dm28c). It was measured through the MTT assay using 0.22 mg mL^{-1} phenazine metosulfate (as an electron carrier).[39] *T. cruzi* epimastigote (Dm28c strain), from the authors own collection (Programa de Farmacología Molecular y Clínica, Facultad de Medicina, Universidad de Chile, Santiago, Chile) were grown at 28 °C in Diamond's monophasic medium, as reported earlier, but replacing blood with 4 µM hemin.[40] Fetal calf serum was added to a final concentration of 5%. In this colorimetric assay for testing the trypanocidal activity, the coumarin derivatives were dissolved in DMSO and were added to 3×10^6 parasites mL^{-1} at 10 µM final concentrations in RPMI 1640 culture medium for 24 h at 28 °C.

DMSO final concentration was less than 0.1% v/v. Likewise, Nifurtimox was added as a positive control. Tetrazolium salt was added at a final concentration of 0.5 mg mL^{-1}, incubated at 28°C for 4 h and then solubilized with 10% SDS/0.1 mM HCl and incubated overnight. After incubation, the number of viable

parasites was determined by absorbance measures at 570 nm in a multiwell plate reader (Asys Expert Plus). Untreated parasites were used as controls (100% of viability). Results are reported as the percentage of non-viable epimastigotes regarding the control (parasite in culture medium).

Trypomastigote stage viability study

Vero cells were infected with Dm28c trypomastigotes at a 1:3 (cell:parasite) ratio. *T. cruzi* trypomastigotes were initially obtained from primary cultures of peritoneal macrophage from chagasic mice. Vero cells were cultured in 5% fetal bovine serum supplemented RPMI 1640 medium in humidified air with 5% CO_2 at 37 °C. Vero cell cultures were then infected with trypomastigotes and incubated at 37 °C in humidified air and 5% CO_2 for 5–7 days. After that time, the culture medium was collected, centrifuged at 500 × g for 5 min, and the trypomastigote-containing pellet was re-suspended in free-serum RPMI 1640 and penicillin–streptomycin at a final density of 1×10^7 parasites/mL. Trypomastigote viability assays were performed using the MTT reduction method as described previously. 1×10^7 parasites/ mL were incubated in free-serum RPMI 1640 culture medium at 37 °C, over 24 h with or without the studied compounds. An aliquot of the parasite suspension was extracted and incubated in a 96-well flat-bottom plate and MTT was added at a final concentration of 0.5 mg/mL using 0.22 mg mL^{-1} phenazine metosulfate (as an electron carrier), incubated at 28 °C during 4 h and then made soluble with 10% SDS–0.1 mM HCl and incubated overnight. Formazan formation was measured at 570 nm, with a reference wavelength at 690 nm, in a multiwell plate reader (Asys Expert Plus). Untreated parasites were used as controls (100% viability). Results are reported as the percentage of non-viable parasites regarding the control (parasite in culture medium).

Acknowledgments

The authors thank University of Santiago de Compostela. M.J.M. thanks to the Xunta de Galicia for the postdoctoral grant ED481B 2014/086-0. S.V.R. thanks to the Xunta de Galicia for the postdoctoral grant ED481B 2014/027-0. The authors thank FONDECYT 1150175 and M.L. thanks to FONDECYT postdoctoral 3160022.

References and notes

1 Rassi, A. Jr.; Rassi, A.; Marcondes de Rezende, J. *Infect. Dis. Clin. North Am.***2012**, *26*, 275.
2 Nunes, M. C.; Dones, W.; Morillo, C. A.; Encina, J. J.; Ribeiro, A. L. *J. Am. Coll. Cardiol.* **2013**, *62*, 767.
3 Muschietti, L.V.; Sülsen, V. P.; Martino, V. S. *Studies in Natural Products Chemistry*, Elsevier, **2013**, *Chapter 9*.
4 Castro, D.; Boiani, L.; Benitez, D.; Hernández, P.; Merlino, A.; Gil, C.; Olea-Azar, C.; González, M.; Cerecetto, H.; Porcal, W. *Eur. J. Med. Chem.* **2009**, *44*, 5055.
5 Pagano, M.; Demoro, B.; Toloza, J.; Boiani, L.; González, M.; Cerecetto, H.; Olea-Azar, C.; Norambuena, E.; Gambino, D.; Otero, L. *Eur. J. Med. Chem.* **2009**, *44*, 4937.
6 Aguilera-Venegas, B.; Olea-Azar, C.; Aran, V. J.; Speisky, H. *Fut. Med. Chem.* **2013**, *5*, 1843.
7 Figueroa-Guiñez, R.; Matos, M. J.; Vazquez-Rodriguez, S.; Santana, L.; Uriarte, E.; Borges, F.; Olea-Azar, C.; Maya, J. D. *Curr. Top. Med. Chem.* **2015**, *15*, 850.
8 Pérez-Cruz, F.; Serra, S.; Delogu, G.; Lapier, M.; Maya, J. D.; Olea-Azar, C.; Santana, L.; Uriarte, E. *Bioorg. Med. Chem. Lett.* **2012**, *22*, 5569.
9 Hamdi, N.; Puerta, M. C.; Valerga, P. *Eur. J. Med. Chem.* **2008**, *43*, 2541.
10 Vazquez-Rodriguez, S.; Figueroa-Guiñez, R.; Matos, M. J.; Olea-Azar, C.; Maya, J. D.; Uriarte, E.; Santana, L. *Med. Chem.* **2016**, *In press*.
11 Iaroshenko, V.O.; Erben, F.; Mkrtchyan, S.; Hakobyan, A.; Vilches-Herrera, M.; Dudkin, S.; Bunescu, A.; Villinger, A.; Sosnovskikh, V. Y.; Langer, P. *Tetrahedron* **2011**, *67*, 7946.
12 Matos, M.J.; Viña, D.; Picciau, C.; Orallo, F.; Santana, L.; Uriarte, E. *Bioorg. Med. Chem. Lett*. **2009**, *19*, 5053.
13 Beillerot, A.; Domínguez, J. C.; Kirsch, G.; Bagrel, D. *Bioorg. Med. Chem. Lett.* **2008**, *18*, 1102.
14 Lin, H. C.; Tsai, S. H.; Chen, C. S.; Chang, Y. C.; Lee, C. M.; Lai, Z. Y.; Lin, C. M.; *Biochem. Pharmacol.* **2008**, ***75***, 1416.
15 Ćavar, S.; Kovač, F.; Maksimović, M. *Food Chem.* **2012**, *133*, 930.
16 Zhang, H. Y.; Wang, L. F. *J. Mol. Struc. THEOCHEM.* **2004**, *673*, 199.
17 Castro, L.; Freeman, B. A. *Nutrition* **2001**, *17*, 161.
18 Matos, M. J.; Pérez-Cruz, F.; Vazquez-Rodriguez, S.; Uriarte, E.; Santana, L.; Borges, F.; Olea-Azar, C. *Bioorg. Med. Chem.* **2013**, *21*, 3900.
19 Thuong, P. T.; Hung, T. M.; Ngoc, T. M.; Ha do, T.; Min, B. S.; Kwack, S. J.; Kang, T. S.; Choi, J. S.; Bae, K. *Phytother. Res*. **2010**, *24*, 101.
20 Figueroa, R.; Matos, M.; Vazquez-Rodriguez, S.; Santana, L.; Uriarte, E.; Olea-Azar, C.; Maya, J. D. Synthesis and evaluation of antioxidant and trypanocidal properties of a selected series of coumarin derivatives. *Fut. Med. Chem.* **2013**, *5*, 1911.
21 Freitas, R. F.; Prokopczyk, I. M.; Zottis, A.; Oliva, G.; Andricopulo, A. D.; Trevisan, M. T. S.; Vilegas, W.; Silva, M. G. V.; Montanari, C. A. *Bioorg. Med. Chem.* **2009**, *17*, 2476.
22 de Alcantara, F. C.; Lozano, V. F.; Vale Velosa, A. S.; dos Santos, M. R. M.; Pereira, R. M. S. *Polyhedron* **2015**, *101*, 165.
23 Kabeya, L.; de Marchi, A. A.; Kanashiro, A.; Lopes, N. P.; da Silva, C. H.; Pupo, M. T.; Lucisano-Valim, Y. M. Bioorg. Med. Chem. **2007**, *15*, 1516.
24 Simić, A.; Manojlović, D.; Šegan, D.; Todorović, M. *Molecules* **2007**, *12*, 2327.
25 Chevion, S.; Roberts, M. A.; Chevion, M. *Free Radic. Biol. Med.* **2000**, *28*, 860.
26 Rodríguez, J.; Olea-Azar, C.; Barriga, G.; Folch, C.; Gerpe, A.; Cerecetto, H.; González, M. *Spectrochim. Acta. A Mol. Biomol. Spectrosc.* **2008**, *70*, 557.
27 Nasr, B.; Abdellatif, G.; Cañizares, P.; Sáez, C.; Lobato, J.; Rodrigo, M. A. *Environ. Sci. Technol.* **2005**, *39*, 7234.
28 Bubnov, M. P.; Teplova, I. A.; Cherkasov, V. K.; Abakumov, G. A. *Eur. J. Inorg. Chem.* **2003**, *2003*, 2519.
29 Kubow, S.; Janzen, E. G.; Bray, T.M. *J. Biol. Chem.* **1984**, *259*, 4447.
30 Le Nest, G.; Caille, O.; Woudstra, M.; Roche, S.; Burlat, B.; Belle, V.; Guigliarelli, B.; Lexa, D. *Inorg. Chim. Acta* **2004**, *357*, 2027.
31 Laurie, V. F.; Zúñiga, M. C.; Carrasco-Sánchez, V.; Santos, L. S.; Cañete, A.; Olea-Azar, C.; Ugliano, M.; Agosin, E. *Food Chem.* **2012**, *131*, 1510.
32 Vazquez-Rodriguez, S.; Figueroa-Guiñez, R.; Matos, M. J.; Santana, L.; Uriarte, E.; Lapier, M.; Maya, J. D.; Olea-Azar, C. *Med. Chem. Commun*. **2013**, *4*, 993.
33 Pérez-Cruz, F.; Vazquez-Rodriguez, S.; Matos, M. J.; Herrera-Morales, A.; Villamena, F.; Das, A.; Gopalakrishnan, B.; Olea-Azar, C.; Santana, L.; Uriarte, E. *J. Med. Chem.* **2013**, *56*, 6136.
34 Heim, K. E.; Tagliaferro, A. R.; Bobilya, D. J. *J. Nutr. Biochem.* **2002**, *13*, 572.
35 Díaz-Urrutia, C.A.; Olea-Azar, C.; Zapata, G.A.; Lapier, M.; Mura, F.; Aguilera-Venegas, B.; Arán, V.J.; López-Múñoz, R.A.; Maya, J.D. *Spectrochim. Acta A Mol. Biomol. Spectrosc.* **2012**, *95*, 670.
36 Ćavar, S.; Kovač, F.; Maksimović, M. *Food Chem.* **2009**, *117*, 135.
37 Matos, M. J.; Mura, F.; Vazquez-Rodriguez, S.; Borges, F.; Santana, L.; Uriarte, E.; Olea-Azar, C. *Molecules* **2015**, *20*, 3290.
38 Mosmann, T. *Methods* **1983**, *65*, 55.

39 Bisby, R.H.; Brooke, R.; Navaratnam, S. *Food Chem.* **2008**, *108*, 1002.

40 Vieites, M.; Otero, L.; Santos, D.; Figueroa-Guiñez, R.; Norambuena, E.; Olea-Azar, C.; Aguirre, G.; Cerecetto, H.; González, M.; Morello, A.; Maya, J.D.; Garat, B.; Gambino, D. *J. Inorg. Biochem.* **2008**, *102*, 1033.